Binding of Copper(II) to the Cyclic Octapeptide Patellamide D

Anna L. van den Brenk,[1a] David P. Fairlie,[1b] Graeme R. Hanson,*[,1c] Lawrence R. Gahan,[1a] Clifford J. Hawkins,[1a] and Alun Jones[1b]

Department of Chemistry, 3D Centre, and Centre for Magnetic Resonance, The University of Queensland, Brisbane, Australia 4072

Received November 2, 1993®

Patellamide D ($patH_4$), a cyclic octapeptide from the ascidian *Lissoclinum patella*, with two oxazoline and two thiazole rings, has the 24-azacrown-8 macrocyclic structure. The cyclic octapeptide forms multiple mononuclear copper(II) complexes in which there are three nitrogen ligating atoms, arising from a deprotonated amide and oxazoline and thiazole rings, coordinated to the copper(II) ion. The multiple mononuclear copper(II) complexes can be ascribed to different metal binding sites in $patH_4$; there are four in the asymmetric $patH_4$ molecule and the binding of different ligands (Cl^- or H_2O) to the fourth equatorial coordination site. Patellamide D also forms three binuclear copper(II) complexes ($[Cu_2(patH_2)]^{2+}$, $[Cu_2(patH_2)(OH)]^+$, and $[Cu_2(patH_2)(CO_3)]$) in which each copper(II) ion is coordinated by three nitrogen ligating atoms from a deprotonated amide and oxazoline and thiazole rings. The remaining coordination sites may be occupied by either Cl^- or H_2O in the first two complexes, while carbonate is assumed, on the basis of X-ray crystallography presented in a future paper, to bridge the two copper(II) ions in the third complex. Electronic absorption, circular dichroism, electron paramagnetic resonance, and mass spectra are reported as a function of the concentration of base added to the copper(II) patellamide solutions.

Introduction

In the marine kingdom many strong ligating groups have been found in compounds isolated from most phyla, including the phylum Chordata, to which the Ascidiacea belong.[2] Families of cyclic peptides including depsipeptides have been isolated from species of the Ascidiacea and have been found to possess significant antineoplastic and antiviral activity.[3,4] Members of the family of cyclic peptides, patellamides, which have the 24-azacrown-8 macrocyclic structure **1** (Chart 1) have been isolated from the aplousobranch ascidian *Lissoclinum patella*.[3,5-7]

The oxazoline and thiazole rings result from the condensation of threonine (serine for patellamide A) and cysteine with adjacent residues. The X-ray crystal structure of ascidiacyclamide (**1**, $ascidH_4$; $R_1 = R_3 =$ D-val; $R_2 = R_4 =$ L-ile; X = Me[8]) shows that the cyclic peptide chain takes on a saddle-shaped conformation (type II) **2** with the thiazole and oxazoline rings located alternately at each corner of the rectangular ring with the eight nitrogens pointing toward the interior of the molecule in an optimal arrangement for chelation.[9,10] There are no intramolecular hydrogen bonds. In contrast, the X-ray structure of patellamide D (**1**, $patH_4$; $R_1 =$ D-ala; $R_3 =$ D-phe; $R_2 = R_4 =$ L-ile; X = Me) shows the peptide backbone is folded with a twisted "figure eight" structure (type III) **3** stabilized by two transannular N—H···O=C and two transannular N—H···O$^-$ (oxazoline ring) hydrogen bonds.[11]

L. patella has been found to concentrate a range of metals including copper(II) (1.56 ppm, dry weight of *L. patella*, compared to that found in seawater (0.08 ppb and 0.027 ppm measured on the reef crest at high and low tides, respectively)).[12] It is interesting to speculate that these cyclic peptides may be involved in the concentration of metal ions by this ascidian. In order to understand the metal binding properties of these peptides we report, herein, the coordination of copper(II) by patellamide D, investigated by electronic absorption, circular dichroism, electron paramagnetic resonance (EPR)[13] spectroscopy, and electrospray mass spectrometry. A future paper reports an X-ray crystal structure of the binuclear copper(II) ascidiacyclamide complex and its spectroscopic properties in the solid state.[14]

Experimental Section

Materials. Patellamide D was isolated and purified from *Lissoclinum patella* collected from Heron Island on the Great Barrier Reef, Australia.[7] Copper(II) chloride dihydrate (Ajax), copper(II) nitrate trihydrate (BDH), copper(II) triflate (Aldrich), sodium carbonate (BDH), methanol (Mallinckrodt), and anhydrous triethylamine (Aldrich) were of analytical grade and used without further purification. ^{63}Cu-enriched copper(II) chloride was prepared from copper oxide obtained from Oak Ridge National Laboratory, Oak Ridge, TN. Metal analyses of stock solutions of copper(II) chloride were determined on a Varian AA-875 atomic absorption spectrometer. Sodium carbonate enriched with ^{13}C (99%) was purchased from Cambridge Isotope Laboratories, Cambridge, MS.

* Author to whom correspondence should be sent.

® Abstract published in *Advance ACS Abstracts*, April 1, 1994.

(1) (a) Department of Chemistry. (b) 3D Centre. (c) Centre for Magnetic Resonance.

(2) Hawkins, C. J. *Pure Appl. Chem.* **1988**, *60*, 1267.

(3) Ireland, C. M.; Durso, A. R., Jr.; Newman, R. A.; Hacker, M. P. *J. Org. Chem.* **1982**, *47*, 1807.

(4) Rinehart, K. L.; Sakai, R.; Holt, T. G.; Fregeau, N. L.; Perun, T. J.; Seigler, D. S.; Wilson, G. R.; Shield, L. S. *Pure Appl. Chem.* **1990**, *62*, 1277.

(5) Hamamoto, Y.; Endo, M.; Nakagawa, M.; Nakanishi, T.; Mizukawa, K. *J. Chem. Soc., Chem. Commun.* **1983**, 323.

(6) Sesin, D. F.; Gaskell, S. J.; Ireland, C. M. *Bull. Soc. Chim. Belg.* **1986**, *95*, 853.

(7) Degnan, B. M.; Hawkins, C. J.; Lavin, M. F.; McCaffrey, E. J.; Parry, D. L.; van den Brenk, A. L.; Watters, D. J. *J. Med. Chem.* **1989**, *32*, 1349.

(8) Abbreviations: $ascidH_4$, ascidiacyclamide; CD, circular dichroism; EPR, electron paramagnetic resonance; Et, ethyl; LSE, least-squares error parameter; Me, methyl; MeOH, methanol; m/z, mass over charge ratio; $patH_4$, patellamide D; triflate, trifluoromethanesulfonate.

(9) Ishida, T.; Inoue, M.; Hamada, Y.; Kato, S.; Shioiri, T. *J. Chem. Soc., Chem. Commun.* **1987**, 370.

(10) Ishida, T.; Tanaka, M.; Nabae, M.; Inoue, M.; Kato, S.; Hamada, Y.; Shioiri, T. *J. Org. Chem.* **1988**, *53*, 107.

(11) Schmitz, F. J.; Ksebati, M. B.; Chang, J. S.; Wang, J. L.; Hossain, M. B.; van der Helm, D.; Engel, M. H.; Serban, A.; Silfer, J. A. *J. Org. Chem.* **1989**, *54*, 3463.

(12) van den Brenk, A. L.; Gahan, L. R.; Hanson, G. R.; Hawkins, C. J. Unpublished results, 1992.

(13) The International EPR Society is recommending that the acronym EPR rather than ESR be used to describe this technique.

(14) van den Brenk, A. L.; Byriel, K. A.; Fairlie, D. P.; Gahan, L. R.; Hanson, G. R.; Hawkins, C. J.; Jones, A.; Kennard, C. H. L.; Moubaraki, B.; Murray, K. S. *Inorg. Chem.*, in press.

0020-1669/94/1333-2280$04.50/0

Chart 1

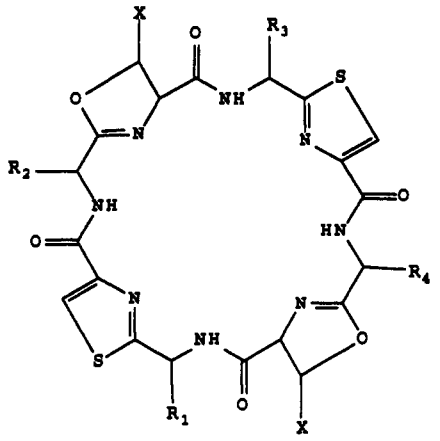

1

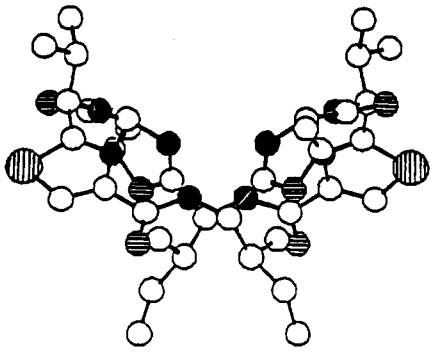

2

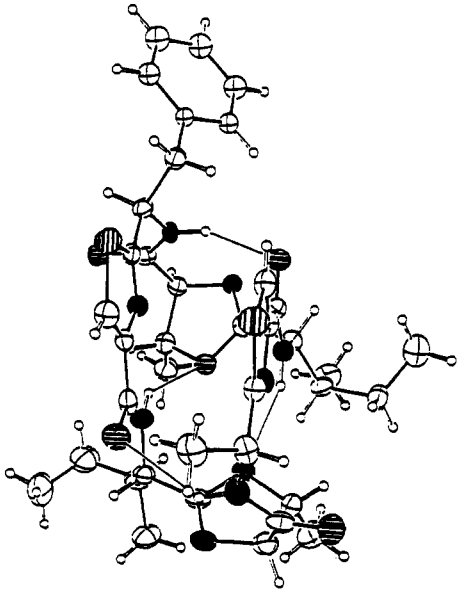

3

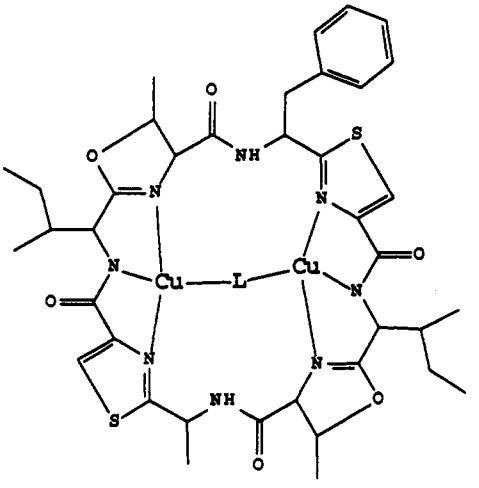

4

(● = N, ◎ = O, ◍ = S, L = CO_3^{2-})

Physical Measurements. Electronic absorption and circular dichroic spectra were measured with a Hewlett Packard 8450A spectrophotometer and a Jobin-Yvon Dichrographe III spectrometer, respectively.

Samples for mass spectrometry were injected into an atmospheric pressure ionization source of an API-111 triple quadrupole mass spectrometer (PE/Sciex, Thornhill, Ontario, Canada). The pneumatically assisted electrospray[15] (Ion Spray[16]) interface was operated at 0.5 kV to generate positive (or protonated) ions. After solvent evaporation,[17] these ions were drawn into the analyzer where they were subjected to an orifice potential difference (OR-RO, 0–200 V). Lower potential differences (0–50 V) typically produced intact molecular ions, while higher values tended to fragment them. Ions were then separated according to their mass over charge ratios by R_f and DC voltages and detected with an electron multiplier by scanning the first quadrupole between m/z = 200–1200 in 6 s with mass resolutions of 0.5 or 0.1 Da. Spectra were subsequently processed on a MAC II FX computer. The peaks in the mass spectra of solutions containing copper(II) patellamide complexes are relatively broad and in some cases very weak (Figures 8, S2 and S6 (supplementary material)). The broad signals arise from isotope distributions and the low-resolution detection system. These factors account for some of the large differences between the experimental and calculated m/z ratios (Table 1). In mass spectra where these weak peaks are more intense the difference between experimental and calculated values is within experimental error.

Multifrequency (Q-band, ~34 GHz; X-band, ~9.2 GHz; S-band, ~4 GHz) EPR spectra, recorded as the first derivative of absorption, were obtained using a Bruker ESP300E EPR spectrometer. Cylindrical TE_{011}, rectangular TE_{102} cavities, and a flexline resonator were used to measure the Q-, X- and S-band EPR spectra, respectively. Versions 3.01 and 3.02 of Bruker's esp300e software were employed for data collection. A flowthrough cryostat in conjunction with a Eurotherm (B-VT-2000) variable-temperature controller provided temperatures of 120–140 K at the sample position in the cavity. Calibration of the microwave frequency and the magnetic field were performed with an EIP 548B microwave frequency counter and a Bruker 035M gaussmeter.

Computer Simulation of EPR Spectra. Simulation of the monomeric copper(II) EPR signal (S), measured as a function of magnetic field (B) and at a constant frequency (ν_c) was performed using eq 1,[18] where the constants, C and a_i, involve experimental parameters and the natural

(15) Yamashita, M.; Fenn, J. B. *J. Phys. Chem.* **1984**, *88*, 4451.
(16) Bruins, A. P.; Covey, T. R.; Henion, J. D. *Anal. Chem.* **1987**, *59*, 2642.
(17) Iribarne, J. V.; Thomson, B. A. *J. Chem. Phys.* **1976**, *64*, 2287.

$$S(\nu_c, B) = C\sum_{i=1}^{2}\sum_{\theta=0}^{\pi/2}\sum_{M_I=-3/2}^{3/2}\sum_{M_N=-3or-4}^{3or4}\sum_{M_H=-1/2}^{1/2} a_i b(M_N)\overline{g_1}^2 f(\nu_c - \nu_0(B),\sigma_\nu)\Delta\cos\theta \quad (1)$$

abundance of the two copper isotopes (^{63}Cu and ^{65}Cu), respectively. The $b(M_N)$ values are the binomial coefficients for magnetically equivalent nitrogens, viz. 1:3:6:7:6:3:1 for three nitrogens and 1:4:10:16:19:16:10:4:1 for four nitrogens. $\overline{g_1}^2$ is the powder averaged expression for the transition probability,[19] and f, the Gaussian line shape function. In f, $\nu_0(B)$ is the actual energy difference between the energy levels and is evaluated with second-order perturbation theory.[20,21] The fundamental reason for using eq 1 is given elsewhere.[22]

The line width, σ_ν, as a function of the polar angle θ, required for randomly orientated (frozen solution) spectral simulations, is assumed to behave in a manner analogous to that for hyperfine structure, viz:

$$\sigma_\nu^2 = \sum_{i=\parallel,\perp} g_i^2 l_i^2 \sigma_i^2 \quad (2)$$

where l_i are the direction cosines relating the applied magnetic field to the principal g axes ($i = \parallel, \perp$). Correlated g- and A-strain[23] in frequency space[22] was used to calculate the actual line width (σ_i, $i = \parallel, \perp$) as a function of ($\nu_0(B)$) and the nuclear spin quantum number M_I.

$$\sigma_i^2 = \sigma_{R_i}^2 + [(\Delta g_i/g_i)\nu_0(B) + \Delta A_i M_I]^2 \quad (3)$$

The σ_{R_i}'s are residual line widths due to dipolar broadening and/or unresolved metal and ligand hyperfine interactions, while ($\Delta g_i/g_i$) and ΔA_i are the half-widths of the strain-induced distributions of the g- and A-values. A unique set of line width parameters cannot be determined for resonances in which metal hyperfine coupling is unresolved.

Computer simulations of the EPR spectra arising from mononuclear copper(II) complexes were refined using an automatic nonlinear least-squares fitting program epr50fit.f running on a SUN SPARCstation 10/30 workstation.

Determinations of the g and hyperfine matrices and the relative orientation of the two copper(II) sites from the EPR spectra of the dipole–dipole-coupled binuclear copper(II) complexes were accomplished by simulating the $\Delta M_s = \pm 1$ and $\Delta M_s = \pm 2$ resonances with the Fortran programs dissim.f and gndimer.f[24] on the SUN workstation. To date the effect of g- and A-strain on the line widths has not been incorporated into these programs. Consequently, the quality of the simulations is not expected to be as high as those for mononuclear copper(II) complexes; however, reproduction of the resonance field positions was attainable.

The quality of the final simulated spectrum can be estimated from the least-squares error parameter (LSE).[25] Spectral subtractions and comparisons and the determination of LSE were carried out with the EPR software package EPR_PLOT running on the University of Queensland Prentice Computer Centre's VAX 8550 computer.

$$\mathrm{LSE} = \sum_{i=1}^{\mathrm{Npts}} (E_i/I_E - S_i/I_S)^2/\mathrm{Npts} \quad (4)$$

where I_E and I_S are the normalization factors (doubly integrated intensities) and Npts is the number of points in both the simulated (S) and the experimental (E) spectra.

Results and Discussion

The absorption spectrum of patellamide D in methanol consists of a strong absorbance in the ultraviolet region at 236 nm (ϵ, 14 400 M^{-1} cm^{-1}) due to the various organic chromophores present. The CD spectrum in methanol has a positive Cotton effect at 252 nm ($\Delta\epsilon$, +18 M^{-1} cm^{-1}). An electrospray mass spectrum of patH$_4$ (Table 1) reveals peaks attributable to simple cation adducts (H^+, Na^+) of the unfragmented molecular ion. The absence of any EPR signals, or metal ion adducts in the mass spectrum of patH$_4$, excludes the presence of any radicals or metal ions associated with this cyclic octapeptide in its isolated form.

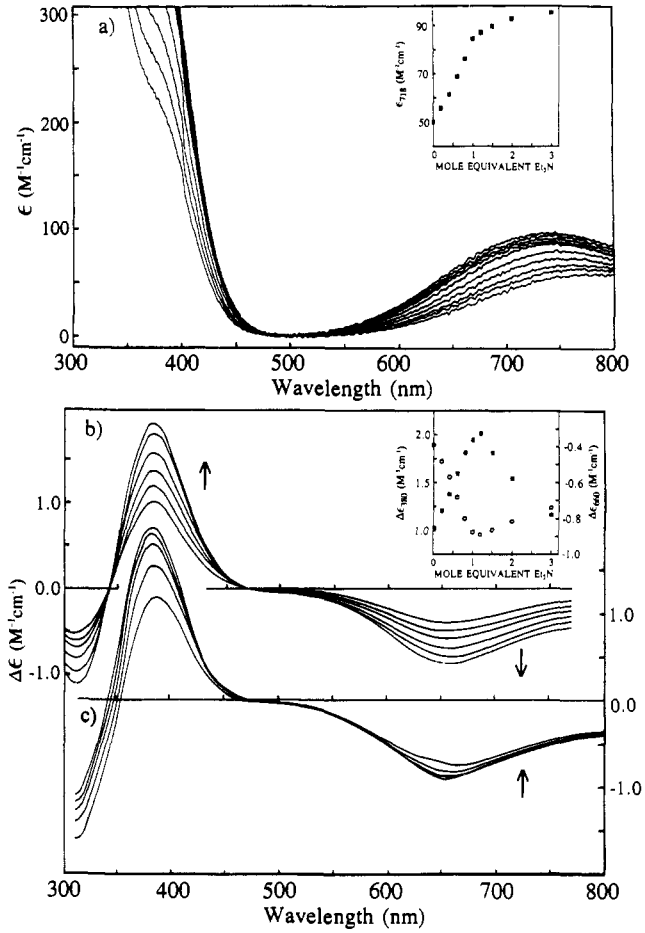

Figure 1. Spectral titrations of a methanolic solution containing patH$_4$ and 1 equiv of copper(II) chloride with triethylamine: (a) Electronic absorption titration (0–3 equiv of base); (b) CD titration (0–1 equiv of base); (c) CD titration (1–3 equiv of base). The insets show plots of the titrations at single wavelengths where ■ corresponds to the ϵ_{718} (M^{-1} cm^{-1}) and $\Delta\epsilon_{380}$ (M^{-1} cm^{-1}) axes and ○ corresponds to the $\Delta\epsilon_{660}$ (M^{-1} cm^{-1}) axis.

Electronic absorption and CD spectral titrations of patH$_4$ with 3 equiv of triethylamine in methanol as a function of copper(II) concentration show a clear end point after the addition of 2 equiv of copper(II) indicating that a maximum of two copper(II) ions coordinate to patellamide D. It should be emphasized that all of the following complexation experiments involving patH$_4$ and copper(II) were performed with milligram quantities of patH$_4$ as only limited quantities of *L. patella* were collected.

Monomeric Copper(II) Patellamide D Complexes. The absorption and CD spectra of patH$_4$ in methanol in the presence of 1 equiv of copper(II) chloride are shown in Figure 1a as a function of added triethylamine. In the absence of base, the titration curves (insets to Figure 1a,b) and the EPR spectrum (Figure S1) indicate that a mononuclear copper(II) complex is approximately 60% formed, a consequence of metal-assisted amide deprotonation.[26] The titration curve for 718 nm, depicted in the inset, shows an initial increase in the absorbance of the copper(II) d–d bands followed by a plateau region after the

(18) Dougherty, G.; Pilbrow, J. R.; Skorobogaty, A.; Smith, T. D. *J. Chem. Soc., Faraday Trans. 2* **1985**, *81*, 1739.
(19) Pilbrow, J. R. *Mol. Phys.* **1969**, *16*, 307.
(20) Freeman, T. E. Ph.D. Thesis, Monash University, Australia, 1973.
(21) Lin, W. C. *Mol. Phys.* **1973**, *25*, 247.
(22) (a) Pilbrow, J. R. *J. Magn. Reson.* **1984**, *58*, 186. (b) Pilbrow, J. R. *Transition Ion Electron Paramagnetic Resonance*; Clarendon Press: Oxford, U.K., 1990.
(23) (a) Froncisz, W.; Hyde, J. S. *J. Chem. Phys.* **1980**, *73*, 3123. (b) Hyde, J. S.; Froncisz, W. *Annu. Rev. Biophys. Bioeng.* **1982**, *11*, 391. (c) Basosi, R.; Antholine, W. E.; Hyde, J. S. *Biol. Magn. Reson.* **1993**, *13*, 103.
(24) Smith, T. D.; Pilbrow, J. R. *Coord. Chem. Rev.* **1974**, *13*, 173.
(25) Martinelli, R. A.; Hanson, G. R.; Thompson, J. S.; Holmquist, B.; Pilbrow, J. R.; Auld, D. S.; Vallee, B. L. *Biochemistry* **1989**, *28*, 2251.
(26) Sigel, H.; Martin, R. B. *Chem. Rev.* **1982**, *82*, 385.

Table 1. Electrospray Mass Spectral Data for Patellamide D and Its Copper Complexes in Methanol[a]

species	m/z[b] exptl	calcd
Patellamide D		
$[patH_4H]^+$	777.8	778.0
$[patH_4Na]^+$	799.0	800.0
$[patH_4(NEt_3H)]^+$	874.2	879.2
Mononuclear Copper(II) Patellamide D Complexes		
$[Cu(patH_3)]^+$	838.2	839.5
$[Cu(patH_3)(H_2O)]^+$	857.4	857.5
$[Cu(patH_3)ClNa]^+$	897.4	898.0
$[Cu(patH_3)Cl(NEt_3H)]^+$	975.8	977.2
Binuclear Copper(II) Patellamide D Complexes		
$[Cu_2(patH)]^+$	900.5	901.0
$[Cu_2(patH_2)(OH)]^+$ or $[Cu_2(patH)(H_2O)]^+$	918.5	919.1
$[Cu_2(patH_2)Cl]^+$	936.0	937.5
$[Cu_2(patH)(CO_2)]^+$	945.0	945.0
$[Cu_2(patH_2)Cl(H_2O)]^+$	952.2	955.5
$[Cu_2(patH_2)(CO_3)H]^+$	962.5	963.1
$[Cu_2(patH_2)Cl(H_2O)_2]^+$	973.2	973.5
$[Cu_2(patH_2)(CO_3)Na]^+$	984.5	985.0
$[Cu_2(patH_2)(CO_3)(NEt_3H)]^+$	1062.0	1064.3

[a] Differences between the experimental and calculated m/z ratios greater than 1 are due to the relatively weak and/or broad signals, the latter arising from isotope distributions and the low-resolution detection system. Better agreement was observed in mass spectra where the signals were more intense. [b] Calculated mass over charge ratios were determined using naturally abundant isotopes.

addition of 1 equiv of base. The electronic absorption and CD spectral characteristics for the mononuclear copper(II) complex ($[Cu(patH_3)]^+$) are as follows: λ_{max}, 746 nm; ϵ, 89.2 M^{-1} cm^{-1}; λ_{max}, 383, 650 nm; $\Delta\epsilon$, +1.96, −0.89 M^{-1} cm^{-1}. The CD titration (Figure 1b) between 0 and 1 equiv of base reveals isosbestic points on the baseline at 342 and 468 nm consistent with one dominant optically active copper(II) patellamide complex. In contrast, the EPR studies described below, and the absence of an isosbestic point in the electronic absorption spectral titration, indicate the presence of multiple copper(II) species. Since there are only minor differences in the EPR parameters for the multiple mononuclear copper(II) patellamide complexes (described below), it is not surprising that the less sensitive CD spectra only reveal a single optically active species. A mass spectrum of a solution containing 1 equiv of copper(II) chloride, $patH_4$, and triethylamine (Figure S2) in methanol yields the peaks listed in Table 1, which also lists their assignments. The presence of a chloride ion in the peak attributed to $[Cu(patH_3)Cl(NEt_3H)]^+$ was distinguished from two water molecules by a comparison of the theoretical isotope distributions of these two species with the experimental spectrum (Figure S2 and inset). A similar analysis proved the existence of a chloride ion in the peak attributed to $[Cu(patH_3)ClNa]^+$. There were no peaks attributable to methanol adducts.

The mononuclear copper(II) patellamide complex ($[Cu(patH_3)]^+$) was further characterized with EPR spectroscopy. X- and Q-band frozen solution EPR spectra of $[Cu(patH_3)]^+$ are shown in Figure 2a,b, respectively. While the first and second derivative X-band spectra can be simulated assuming a single species (Figure S3), the Q-band spectrum (Figure 2b) reveals five copper hyperfine resonances in the parallel region attributable to two copper(II) species (species 1 and 2). Computer simulation of the spectrum attributable to species 1 with the axial spin Hamiltonian (eq 5) and the g, copper, and ligand hyperfine

$$\mathcal{H} = g_\parallel \beta B_z S_z + g_\perp \beta (B_x S_x + B_y S_y) + A_\parallel S_z I_z + A_\perp (S_x I_x + S_y I_y) + \sum_{i=1}^{3or4} [A_\parallel^N S_z I_z^N + A_\perp^N (S_x I_x^N + S_y I_y^N)] + A_\parallel^H S_z I_z^H + A_\perp^H (S_x I_x^H + S_y I_y^H) \quad (5)$$

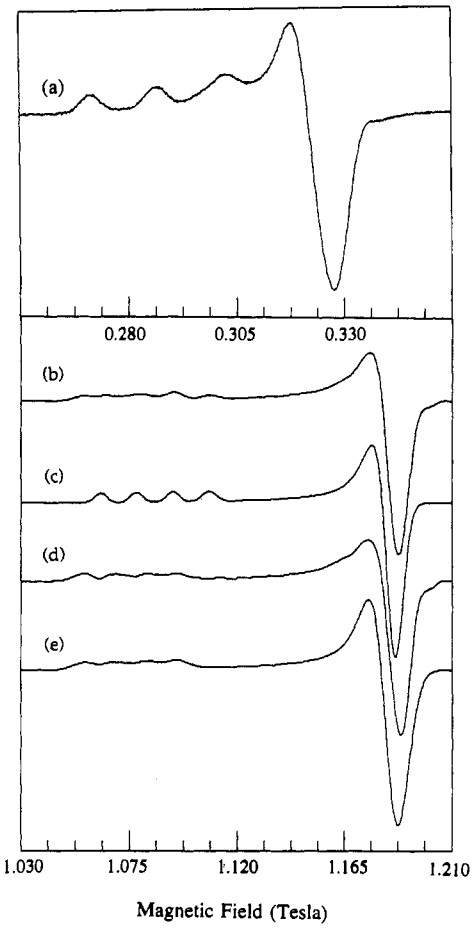

Figure 2. EPR spectra of $[Cu(patH_3)]^+$: (a) X-band EPR spectrum in methanol, ν = 9.2537 GHz; (b) Q-band EPR spectrum in methanol, ν = 34.0194 GHz; (c) computer simulation of species 1; (d) Q-band EPR spectrum of species 2 obtained by subtracting 0.36 of (c) from (b); (e) computer simulation of species 2.

matrices (the latter obtained from S-band spectra; see below) and line width parameters in Tables 2 and 3 yields the spectrum shown in Figure 2c. Using the high-field parallel resonance to monitor the presence of species 1, we were able to obtain the spectrum associated with species 2 (Figure 2d) by subtracting the spectral simulation (Figure 2c) multiplied by 0.36 from the experimental spectrum (Figure 2b). A computer simulation of the spectrum associated with species 2 is shown in Figure 2e. A comparison of the experimental Q-band EPR spectrum (Figure 2b) with a simulated spectrum (results not shown; LSE = 6.136 × 10^{-4}) obtained by adding Figure 2c multiplied by 0.36 to Figure 2e multiplied by 0.64 demonstrates the reliability of the above analysis. Since the perpendicular region of the Q-band EPR spectrum consisted of only a single broad unresolved resonance, $A_\perp$(Cu), $A_\perp$(N), and $A_\perp$(H) were assumed to be identical to those obtained from the simulation of the X-band EPR spectrum (Table 2) and the line width parameters were allowed to vary to obtain quality simulations.

The axial g and copper hyperfine matrices of these two species are very similar (Table 2) and are consistent with tetragonally distorted copper(II) sites in which there are three nitrogen ligating atoms coordinated to the copper(II) ion. The origin of species 1 and 2 can be ascribed to (i) the presence of different metal binding sites ($[Cu(patH_3)]^+$ and $[Cu(patH_3')]^+$) in $patH_4$, of which there are four by virtue of the absence of symmetry in $patH_4$, (ii) the binding of different ligands (Cl^- or H_2O) to the fourth equatorial coordination site, or (iii) a combination of these effects. Thus the equilibria describing the formation of $[Cu(patH_3)]^+$ in methanol are suggested to be

Table 2. EPR Parameters for Mononuclear and Binuclear Copper(II) Complexes of Patellamide D

Mononuclear Copper(II) Complexes

complex	g_z	g_x	g_y	A_z(Cu)[a]	A_x(Cu)	A_y(Cu)	$A_\parallel$(N)[b]	$A_\perp$(N)[b]	$A_\parallel$(H)
$[Cu(MeOH)]^{2+}$	2.4235	2.0884	2.0884	119.51	3.32	3.32			
$[Cu(patH_3)]^+$ X-,S-band	2.2600	2.0630	2.0630	149.92	11.34	11.34	12.37	12.63	4.2
species 1	2.2390	2.0550	2.0550	153.66	11.34	11.34	12.37	12.63	4.2
species 2	2.2601	2.0530	2.0530	133.00	11.34	11.34	12.37	12.63	4.2

Binuclear Copper(II) Complexes

complex	g_z	g_x	g_y	A_z(Cu)	A_x(Cu)	A_y(Cu)	ζ^0	η^0	τ^0	r (Å)
$[Cu_2(patH_2)]^{2+}$ [c]	2.242	2.060	2.060	160.0	11.0	11.0	54.74	45.0	0.00	6.8
$[Cu_2(patH_2)(OH)]^+$ [d]	2.300	2.150	2.050	150.0	3.0	3.0	15.00	70.00	40.00	4.8
$[Cu_2(patH_2)(CO_3)]$ [e]	2.267	2.075	2.075	111.0	70.0	70.0	140.00	0.00	0.00	3.7

[a] Units for ^{63}Cu and ligand nitrogen and proton hyperfine coupling constants are 10^{-4} cm^{-1}. [b] Computer simulation based on three magnetically equivalent nitrogen atoms. The principal directions of the ligand nitrogen hyperfine axes are coincident with the g axes. [c] Computer simulation was performed using the similar ion dimer program (gndimer.f). The line widths for the $\Delta M_s = \pm 1$ and ± 2 resonances were σ_z 35.0, 20.0; σ_x 15.0, 22.0; and σ_y 15.0, 22.0 (MHz), respectively. [d] Computer simulation was performed using the dissimilar ion dimer program (dissim.f). Both sites 1 and 2 had identical g and A matrices. The line widths for the $\Delta M_s = \pm 1$ and ± 2 resonances were σ_z 100.0; σ_x 30.0; and σ_y 30.0 (MHz), respectively. [e] Computer simulation was performed using the similar ion dimer program (gndimer.f). The line widths for the $\Delta M_s = \pm 1$ and ± 2 resonances were σ_z 140.0, 23.0; σ_x 30.0, 25.0; and σ_y 30.0, 25.0 (MHz), respectively.

Table 3. Line Width Parameters for Mononuclear Copper(II) Complexes of Patellamide D

complex	$\sigma_{R\parallel}$[a]	$\sigma_{R\perp}$[a]	$\Delta g_\parallel / g_\parallel$	$\Delta g_\perp / g_\perp$	$\Delta A_\parallel$[a]	$\Delta A_\perp$[a]
$[Cu(MeOH)]^{2+}$	17.67	64.09	0.00 795	0.009 68	43.41	157.09
$[Cu(patH_3)]^+$ [b] X-band	17.56	24.28	0.00 372	0.000 49	19.00	39.87
species 1	26.80	29.94	0.00 156	−0.003 03	18.80	40.25
species 2	12.65	11.49	0.00 404	−0.004 05	6.11	2.87

[a] Units for σ_R, $\Delta A_\parallel$, and $\Delta A_\perp$ are MHz. [b] Computer simulation based on three magnetically equivalent nitrogen atoms.

$$[Cu(MeOH)]^{2+} + patH_4 + NEt_3 \rightleftharpoons$$
$$k[Cu(patH_3)H_2O]^+ + l[Cu(patH_3)Cl] + NEt_3H^+ \quad (6)$$
$$\updownarrow \qquad\qquad \updownarrow$$
$$m[Cu(patH_3')H_2O]^+ + n[Cu(patH_3')Cl]$$
$$k + l + m + n = 1$$

A reduction in correlated g- and A-strain at lower microwave frequencies (S-band, 2–4 GHz, and L-band, 1–2 GHz) yields narrower line widths which often allow the observation of ligand hyperfine coupling.[23] Hyde and Froncisz[23a,b] have shown that the optimum microwave frequency for the resolution of ligand hyperfine coupling on the parallel $M_I = -1/2$ hyperfine resonance is approximately 2 GHz. Computer simulation of this resonance often allows the identification of the number and type of ligating atoms (with nonzero nuclear spin) coupled to the electron spin. For instance the major differences between the simulations based on three and four magnetically equivalent nitrogen nuclei are the relative intensities of the ligand hyperfine resonances and the spectral bandwidth (see Experimental Section).[27] An expanded S-band EPR spectrum of ^{63}Cu-enriched $[Cu(patH_3)]^+$ in methanol showing the $M_I = -1/2$ parallel hyperfine resonance is presented in Figure 3a. Resonances labelled with an asterisk in this spectrum (Figure 3a) arise from a small amount of $[Cu(MeOH)]^{2+}$. Computer simulations of the $M_I = -1/2$ parallel hyperfine resonance[28] based on three (Figure 3b, LSE = 1.766×10^{-2}) or four (Figure 3c, LSE = 2.168×10^{-2}) magnetically equivalent nuclei indicate that there are three nitrogen nuclei coordinated to the copper(II) ion. A closer examination of the ligand hyperfine resonances (Figure 3a, labelled with a number sign) reveals a doublet splitting (4.2×10^{-4} cm^{-1}) that is attributed to hyperfine coupling from a single proton (Figure 3d). The most likely sources of this proton coupling are from an equatorially coordinated solvent molecule, an amide, or a methine proton on the patellamide backbone. The extent to which deuterium will exchange with this proton should allow us to distinguish a methine proton from either a solvent molecule or an amide proton. The EPR spectrum of $[Cu(patH_3)]^+$ in fully deuterated methanol (results not shown) revealed virtually no change, indicating that the origin of the proton hyperfine coupling was most likely a methine proton. A two-dimensional HYSCORE spectrum[29] of the perpendicular resonance revealed isotropic proton hyperfine coupling(s) of less

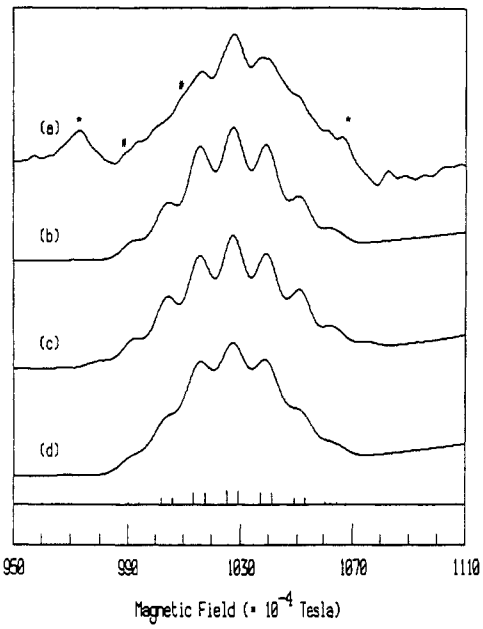

Figure 3. S-band EPR spectra of $[Cu(patH_3)]^+$ showing the parallel $M_I = -1/2$ hyperfine resonance: (a) Experimental spectrum, Fourier smoothed, ν = 3.4758 GHz, where resonances labeled with an asterisk arise from $[Cu(MeOH)]^{2+}$; (b) computer simulation of Figure 3a assuming three magnetically equivalent nitrogen nuclei, LSE = 1.766×10^{-2}; (c) computer simulation of Figure 3a assuming four magnetically equivalent nitrogen nuclei, LSE = 2.168×10^{-2}; (d) computer simulation of Figure 3a assuming three magnetically equivalent nitrogen nuclei and a single proton, LSE = 1.945×10^{-2}.

(27) Rakhit, G.; Antholine, W. E.; Froncisz, W.; Hyde, J. S.; Pilbrow, J. R.; Sinclair, G. R.; Sarkar, B. *J. Inorg. Biochem.* **1985**, *25*, 217.

(28) Although the Q-band EPR spectrum revealed multiple copper(II) species in solution (Figure 2), the computer simulations were performed by assuming a single species, as at S-band frequencies the $M_I = -1/2$ resonance from species 1 and 2 will occur at very similar magnetic fields (ΔB = 0.06 mT).

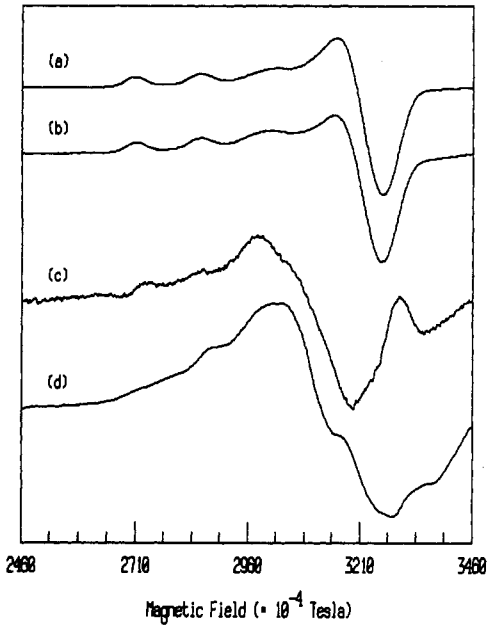

Figure 4. (a) X-band EPR spectrum of a solution containing 1 equiv of copper(II) chloride, patellamide D, and triethylamine in methanol, ν = 9.2538 GHz. (b) Same as for (a) except with 3 equiv of base, ν = 9.2511 GHz. (c) Spectral subtraction {(b) − 0.95([Cu(patH$_3$)]$^+$), (a)} revealing the presence of a small amount of a dipole–dipole-coupled EPR signal. (d) X-band EPR spectrum of a solution containing 1 equivalent of copper(II) nitrate, patellamide D, and triethylamine in methanol, ν = 9.92921 GHz.

than or equal to 4×10^{-4} cm^{-1}. The field dependence of these couplings was found to be consistent with the analysis of the S-band spectrum.

The second derivative X-band EPR spectrum of [Cu(patH$_3$)]$^+$ (Figure S3b) reveals both copper and ligand hyperfine couplings in the perpendicular region. Computer simulation of this spectrum provided the remaining spin Hamiltonian parameters listed in Table 2.

When the concentration of base is increased above 1 equiv (Figure 1c), shifts in the wavelength maxima (from 383 and 650 nm to 386 and 666 nm) and changes in $\Delta\epsilon$ (1.96 and −0.89 M^{-1} cm^{-1} to 1.21 and −0.74 M^{-1} cm^{-1}) are observed. A detailed examination of the EPR spectrum arising from a solution containing the mononuclear copper(II) patellamide complex (Figure 4a) and an additional 2 equiv of base reveals broadening in the perpendicular region with a larger value of $g_\perp$ (Figure 4b).

There are two possible reasons for these observations: first, an increase in g- and A-strain (see Experimental Section) and, second, the presence of a second species. An increase in g- and A-strain can be ruled out as the peak to peak line width ($\Delta B_{pp\perp}$ = 154.0 MHz) remains unchanged. Subtraction of the spectrum (Figure 4a) arising from [Cu(patH$_3$)]$^+$ from this spectrum (Figure 4b) yields a spectrum (Figure 4c) that shows a small proportion of an S = 1 EPR signal arising from a binuclear copper(II) complex ([Cu$_2$(patH$_2$)(OH)]$^+$; see below). This species represents less than 5% of the total Cu(II) present. An X-band EPR spectrum (Figure 4d) of a solution containing patH$_4$, a copper(II) salt containing a noncoordinating anion (NO_3^-), and triethylamine in the ratio of 1:1:1 shows resonances predominantly (greater than 90%) arising from an S = 1 spin system, attributable to a binuclear copper(II) patellamide complex ([Cu$_2$(patH$_2$)(OH)]$^+$; see below and compare Figures 4d and 6d). There is no mass spectral evidence for the coordination of nitrate to copper(II). The existence of a binuclear copper(II) complex implicates at least two distinct copper(II) binding sites in patH$_4$ ([Cu(patH$_3$)]$^+$ and [Cu(patH$_3$′)]$^+$). The spectral differences observed when using copper(II) chloride (Figure 4a–c) versus copper(II) nitrate (Figure 4d) can be interpreted with the aid of the following equilibrium:

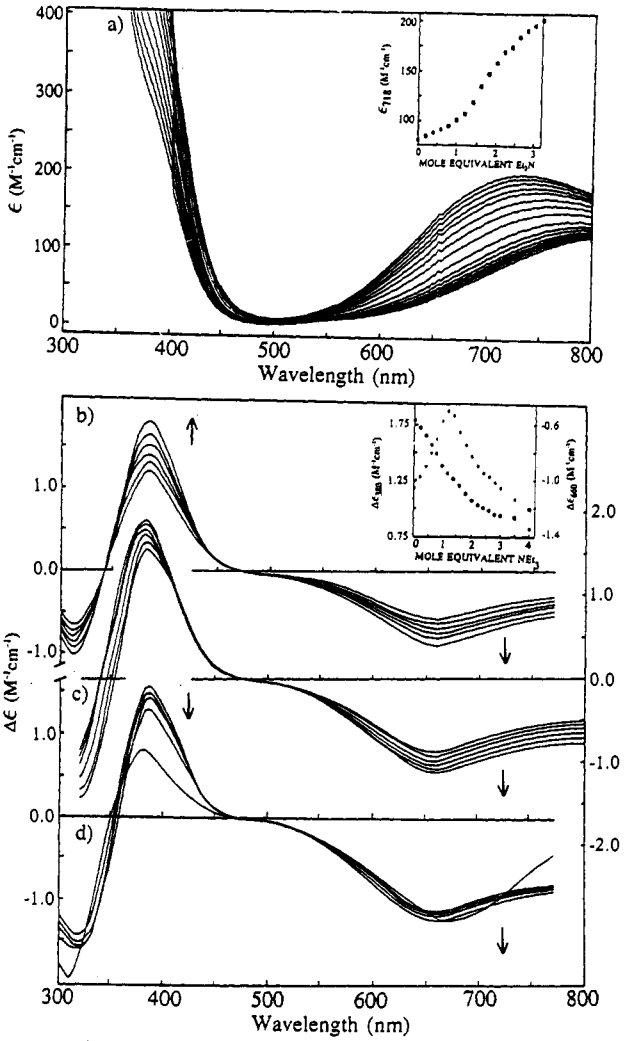

Figure 5. Spectral titrations of a solution containing patH$_4$ and 2 equiv of copper(II) with triethylamine in methanol: (a) Electronic absorption titration, (0–3 equiv of base); (b) CD titration (0–1 equiv of base); (c) CD titration (1–2 equiv of base); (d) CD titration, (2–3, 4 equiv of base). The insets show plots of the titrations at single wavelengths where ■ corresponds to the ϵ_{718} (M^{-1} cm^{-1}) and $\Delta\epsilon_{380}$ (M^{-1} cm^{-1}) axes and ○ corresponds to the $\Delta\epsilon_{660}$ (M^{-1} cm^{-1}) axis.

$$2[Cu(MeOH)]^{2+} + 2patH_4 + 2NEt_3 \rightleftharpoons 2[Cu(patH_3)]^+ + 2NEt_3H^+$$

$$2[Cu(patH_3)]^+ + NEt_3 \rightleftharpoons [Cu_2(patH_2)OH]^+ + NEt_3H^+ + patH_4 \quad (7)$$

In the absence of chloride ions the position of this equilibrium lies to the right-hand side favoring the binuclear copper(II) complex. In contrast, if chloride is present, the predominant species is the mononuclear copper(II) complex, (eq 6), containing chloride as established by mass spectrometry. The above equilibria are also consistent with our mass spectra which show mixtures of patH$_4$, mononuclear and binuclear copper(II) patellamide complexes, and NEt$_3$H$^+$ under most conditions.

Binuclear Copper(II) Patellamide D Complexes. In methanol, the electronic absorption (Figure 5a, inset) and CD (Figure 5b–d, inset) spectral titrations of solutions containing patellamide D and 2 equiv of copper(II) chloride with triethylamine reveal three end points occurring after the addition of 1, 2, and 3 equiv of base, respectively.

(29) van den Brenk, A. L.; Gahan, L. R.; Hanson, G. R.; Höfer, P. Unpublished results, 1993.

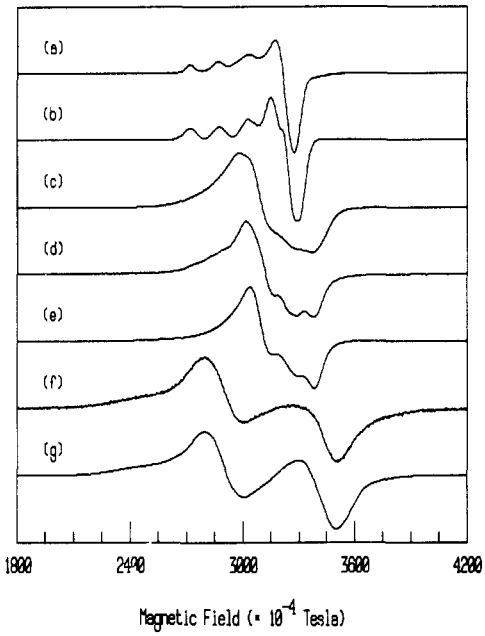

Figure 6. X-band EPR spectra of the $\Delta M_s = \pm 1$ resonances arising from the binuclear copper(II) patellamide D complexes: (a) Experimental spectrum for $[Cu_2(patH_2)]^{2+}$, in methanol prepared with copper(II) chloride, ν = 9.2926 GHz; (b) computer simulation of (a), LSE = 1.099 × 10^{-2}; (c) experimental spectrum for $[Cu_2(patH_2)(OH)]^+$, in methanol prepared with copper(II) chloride, ν = 9.2983 GHz; (d) experimental spectrum for $[Cu_2(patH_2)(OH)]^+$, in methanol prepared with copper(II) nitrate, ν = 9.2991 GHz; (e) computer simulation of (d), LSE = 1.501 × 10^{-2}; (f) experimental spectrum for $[Cu_2(patH_2)(CO_3)]$, in methanol prepared with copper(II) chloride, ν = 9.2858 GHz; (g) computer simulation of (f), LSE = 8.112 × 10^{-3}.

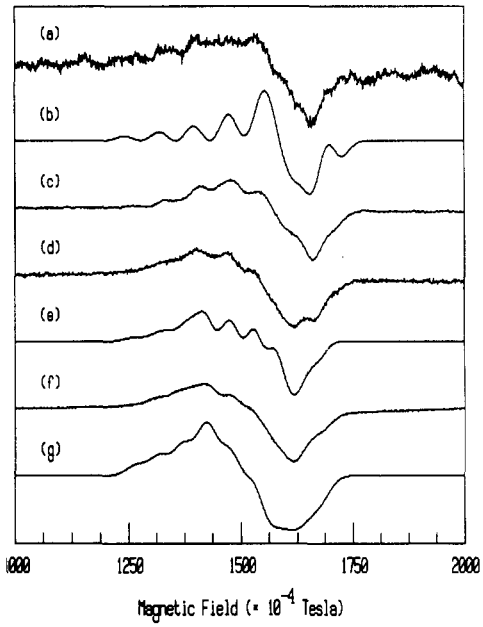

Figure 7. X-band EPR spectra of the $\Delta M_s = \pm 2$ resonances arising from the binuclear copper(II) patellamide D complexes: (a) Experimental spectrum for $[Cu_2(patH_2)]^{2+}$, in methanol prepared with copper(II) chloride, ν = 9.2983 GHz; (b) computer simulation of (a), LSE = 5.457 × 10^{-2}; (c) experimental spectrum for $[Cu_2(patH_2)(OH)]^+$, in methanol prepared with copper(II) chloride, ν = 9.2976 GHz; (d) experimental spectrum for $[Cu_2(patH_2)(OH)]^+$, in methanol prepared with copper(II) nitrate, ν = 9.2991 GHz; (e) computer simulation of (d), LSE = 1.997 × 10^{-2}; (f) experimental spectrum for $[Cu_2(patH_2)(CO_3)]$, in methanol prepared with copper(II) chloride, ν = 9.2858 GHz; (g) computer simulation of (f), LSE = 2.623 × 10^{-2}.

The CD titration from 0 to 1 equiv of triethylamine (Figure 5b) reveals isosbestic points at 342 and 468 nm with $\Delta\epsilon = 0$ M^{-1} cm^{-1}, consistent with the formation of a single optically active copper(II) patellamide D complex. After the addition of 1 equiv of base, the copper(II) patellamide D complex formed has similar CD characteristics (λ_{max}, 383, 652 nm; $\Delta\epsilon$, +1.80, −0.91 M^{-1} cm^{-1}) and EPR parameters ($g_\parallel$, 2.2600; $g_\perp$, 2.0630; $A_\parallel$(Cu), 149.92 × 10^{-4} cm^{-1}; $A_\perp$(Cu), 11.34 × 10^{-4} cm^{-1}) as those found for $[Cu(patH_3)]^+$.

Addition of further base, up to 2 equiv, results in the disappearance of the isosbestic point at 342 nm and a shift in the second isosbestic point from 468 to 492 nm ($\Delta\epsilon$, −0.03 M^{-1} cm^{-1}) (Figure 5c). These changes reflect the presence of two different optically active species, the first of which is $[Cu(patH_3)]^+$. The second species has the following spectral characteristics: λ_{max}, 756 nm; ϵ, 168 M^{-1} cm^{-1}; λ_{max}, 388, 658 nm; $\Delta\epsilon$, +1.57, −1.14 M^{-1} cm^{-1}. The magnitudes of ϵ and $\Delta\epsilon$ are approximately twice that observed for $[Cu(patH_3)]^+$ indicating the second optically active species is a binuclear copper(II) patellamide complex ($[Cu_2(patH_2)]^{2+}$) in which both copper(II) ions are coordinated by three nitrogen atoms, one each from a deprotonated amide, an oxazoline ring, and a thiazole ring. Increasing the base to 3 equiv produces small changes in the electronic absorption and CD spectra (λ_{max}, 734 nm; ϵ, 199 M^{-1} cm^{-1}; λ_{max}, 387, 660 nm; $\Delta\epsilon$, +1.30, −1.25 M^{-1} cm^{-1}) (Figure 5d). After the addition of approximately 3 equiv of base, formation of a blue-green precipitate causes dispersion in the electronic absorption spectra. CD is not as sensitive as electronic absorption spectroscopy to dispersion and consequently will yield superior results at higher concentrations of base. After addition of 4 equiv of base (Figure 5d) the wavelength maxima and delta extinction coefficients have shifted slightly (λ_{max}, 380, 670 nm; $\Delta\epsilon$, +0.81, −1.21 M^{-1} cm^{-1}; Figure 5d). Upon standing for at least 2 or 3 days, samples with either 3 or 4 equiv of base produce a solution that is stable over 6 months and has the following spectral characteristics: λ_{max}, 716 nm; ϵ, 215 M^{-1} cm^{-1}; λ_{max}, 368, 680 nm; $\Delta\epsilon$, +0.821, −1.23 M^{-1} cm^{-1}.

The EPR spectrum of $[Cu_2(patH_2)]^{2+}$ (Figures 6a and 7a) reveals resonances around 300 and 150 mT, the latter being extremely weak. Although the spectrum (Figure 6a) could be interpreted as arising from a monomeric copper(II) complex ($[Cu(patH_3)]^+$) with a single unpaired electron ($S = {}^1/_2$), the absence of resonances associated with $[Cu(MeOH)]^{2+}$ indicates that the 2 equiv of copper(II) are bound to patellamide D forming a binuclear complex. The question arises, how can an $S = {}^1/_2$ like spectrum be obtained from a binuclear copper(II) complex with $S = 1$? The spin Hamiltonian describing a spin-coupled system (eq 8) includes an interaction Hamiltonian ($\mathcal{H}_{int}$) consisting of isotropic exchange and dipole–dipole terms, in addition to the individual spin Hamiltonians ($\mathcal{H}_1$, $\mathcal{H}_2$) for each ion.

$$\mathcal{H} = \mathcal{H}_1 + \mathcal{H}_2 + \mathcal{H}_{int}$$

$$\mathcal{H}_{int} = \mathcal{H}_{ex} + \mathcal{H}_{dip}$$

$$\mathcal{H}_{ex} = \mathbf{J}\cdot\mathbf{S}_1\cdot\mathbf{S}_2$$

$$\mathcal{H}_{dip} = \mathbf{S}_1\cdot\mathbf{J}\cdot\mathbf{S}_2 \qquad (8)$$

In order to eliminate the coupling between the two copper(II) ions, $\mathcal{H}_{int}$ needs to be reduced to zero. When exchange coupling is negligible, $\mathcal{H}_{int}$ is dominated by the dipole–dipole interaction. An examination of the second-rank dipole–dipole coupling tensor (eq 9) for a similar ion copper(II) dimer[24] reveals that each ofthe elements $J_{ij,i,j=x,y,z}$ is inversely proportional to the internuclear distance cubed.[24] Thus increasing the copper(II)–copper(II) distance to greater than 10 Å would effectively reduce this interaction to zero. However, the cyclic octapeptide patellamide D sets an upper limit for the internuclear copper(II)–copper(II)

distance of approximately 7 Å, which would be expected to yield a typical $S = 1$ dipole–dipole-coupled EPR spectrum. A closer examination of this tensor (eq 9) reveals that by choosing the

$$J_{xx} = g_x^2(1 - 3\sin^2\eta\sin^2\xi)\beta_r$$

$$J_{yy} = g_y^2(1 - 3\cos^2\eta\sin^2\xi)\beta_r$$

$$J_{zz} = g_z^2(1 - 3\cos^2\xi)\beta_r$$

$$J_{xy} = J_{yx} = -3g_xg_y\sin^2\xi\sin\eta\cos\eta\,\beta_r$$

$$J_{xz} = J_{zx} = -3g_xg_z\sin\xi\cos\xi\sin\eta\,\beta_r$$

$$J_{yz} = J_{zy} = -3g_yg_z\sin\xi\cos\xi\cos\eta\,\beta_r$$

$$\beta_r = \beta^2/r^3 \qquad (9)$$

angles ξ and η to be 54.7 and 45.0° the diagonal elements J_{xx}, J_{yy}, and J_{zz} are equal to zero. Although the off-diagonal elements are not equal to zero, their effect on the spectrum can be minimized by increasing the internuclear copper(II)–copper(II) distance.

A computer simulation (gndimer.f) of Figure 6a with $\mathcal{H}_{dip}$ (eq 8), the g and A matrices for $[Cu(patH_3)]^+$ (Table 2), the above values for the angles ξ and η, and an internuclear distance of 6.8 Å yields the spectrum shown in Figure 6b, with LSE = 1.099×10^{-2}. These parameters were also used to predict the presence and spectral line shape of the $\Delta M_s = \pm 2$ resonances (Figure 7b), which were found to be similar (LSE = 5.457×10^{-2}) to the extremely weak experimentally observed resonances (Figure 7a).

A comparison of the double integrals (DI)[30] for the $\Delta M_s = \pm 1$ resonances arising from this binuclear copper(II) complex ($S = 1$, $DI_{exp,sim} = 0.3034, 225.3$) and the mononuclear $[Cu(patH_3)]^+$ complex ($S = {}^1/_2$, $DI_{exp,sim} = 0.1368, 82.17$) shows that, within experimental error, the ratios $(DI_{S=1}/DI_{S=1/2})_{exp,sim} = 2.22, 2.74$ are approximately the expected two is to one. The relatively poor simulation of the binuclear complex, as judged by the LSE value (1.099×10^{-2}), a consequence of the line width model employed in gndimer.f, readily explains the large value of 2.74 for $DI_{S=1}/DI_{S=1/2}$. In contrast the ratio of double integrals for the $\Delta M_s = \pm 2$ and ± 1 resonances ($DI_{\Delta M_S=\pm 2}/DI_{\Delta M_S=\pm 1}$) is 9.52×10^{-4}, clearly showing that the dipole–dipole interaction is indeed very close to zero. This is even more apparent when we compare this ratio with similar ratios obtained from spectra for other dipole–dipole-coupled binuclear copper(II) complexes, for example the spectra shown in Figures 7d, 6d and 7f, 6f, $DI_{\Delta M_S=\pm 1} = 4.39 \times 10^{-3}$ and 3.36×10^{-2}, respectively.

Increasing the concentration of base to 3 equiv produces the EPR spectra shown in Figures 6c and 7c attributable to $\Delta M_s = \pm 1$ and ± 2 transitions from a dipole–dipole-coupled $S = 1$ spin system. Although we could simulate (dissim.f) the $\Delta M_s = \pm 1$ resonances (Figure S4) with the dipole–dipole spin Hamiltonian (eq 8) and the parameters listed in Table 2, we were unable to reproduce the spectral line shape of the $\Delta M_s = \pm 2$ resonances. Replacement of copper(II) chloride with copper(II) nitrate produced EPR spectra (Figures 6d and 7d) which had smaller line widths in the $\Delta M_s = \pm 1$ region and a different line shape in the $\Delta M_s = \pm 2$ region. Computer simulation (dissim.f) of both the $\Delta M_s = \pm 1$ and ± 2 resonances with the dipole–dipole spin Hamiltonian (eq 8) and the parameters in Table 2 yields the spectra shown in Figures 6e (LSE = 1.501×10^{-2}) and 7e (LSE = 1.997×10^{-2}). The inability to simulate Figures 6c and 7c clearly indicates the presence of multiple binuclear copper(II) complexes when copper(II) chloride is used as a starting material. Interestingly the internuclear copper(II)–copper(II) distance (Table 2) has decreased from 6.8 to 4.8 Å indicating that the two halves of the patellamide D molecule are folding in such a way as to bring the two copper(II) ions closer together.

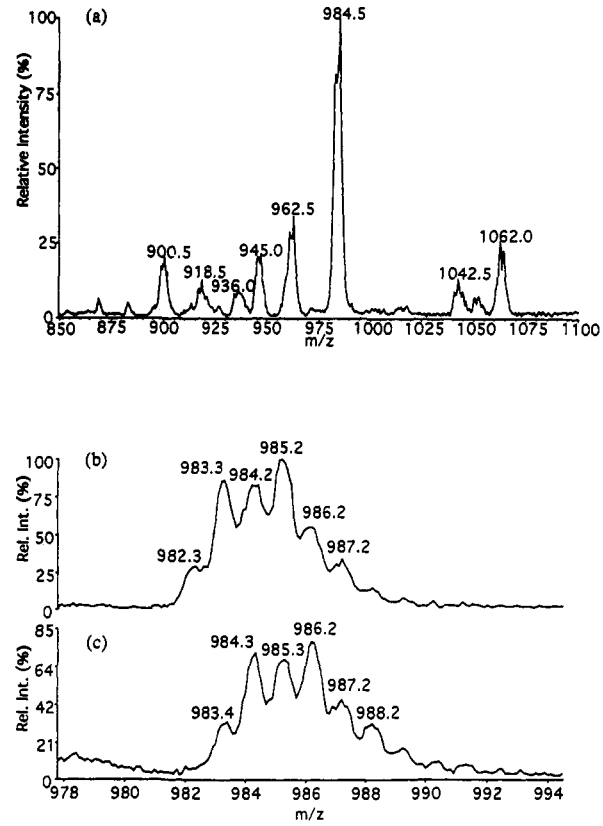

Figure 8. Mass spectra of the binuclear copper(II) patellamide D complexes: (a) Mass spectrum of a solution containing 2 equiv of copper(II) chloride, 1 equiv of patellamide D, and 3 equiv of triethylamine; (b, c) expansions of the mass spectra of the peaks attributed to the sodium adducts of $[Cu_2(patH_2)(^{12}CO_3)]$ (b) and $[Cu_2(patH_2)(^{13}CO_3)]$ (c).

Adding more base, up to 4 equiv, and leaving the solution for at least 1 day produces the EPR spectra shown in Figures 6f and 7f. In contrast to the spectra shown in Figures 6c, 6d and 7c, 7d, the line shape and resonant field positions are unaffected upon replacing copper(II) chloride (Figures 6f and 7f) with copper(II) nitrate (Figure S5). Leaving either sample to stand for a 6-month period also has no effect on the spectral line shape, indicating that this binuclear copper(II) complex is the most thermodynamically stable species in solution. Computer simulation (gndimer.f) of the $\Delta M_s = \pm 1$ and ± 2 resonances with the dipole–dipole spin Hamiltonian (eq 8) and the parameters listed in Table 2 produces the spectra shown in Figures 6g (LSE = 8.112×10^{-3}) and 7g (LSE = 2.623×10^{-2}). Again the copper(II)–copper(II) internuclear distance was found to be shorter, 3.7 Å.

Mass spectra of reaction mixtures containing copper(II) chloride, triethylamine, and $patH_4$ in the ratios $2{:}\geq 2{:}1$ are relatively simple. With 3 equiv of base (Figure 8a, Table 1) peaks attributable to $[Cu_2(patH)]^+$, $[Cu_2(patH)(H_2O)]^+$, $[Cu_2(patH_2)Cl]^+$, $[Cu_2(patH)(CO_2)]^+$ and H^+, Na^+, or NEt_3H^+ adducts of the binuclear copper(II) complex $[Cu_2(patH_2)(CO_3)]$ were observed. Peaks below 750 Da can be assigned to numerous adducts of triethylamine. The peak with $m/z = 945.0$ was assigned to $[Cu_2(patH)(CO_2)]^+$ as the presence of two sodium ions would have produced a multiply charged cation $[Cu_2(patH)Na_2]^{3+}$ and hence it would have an m/z of 315 and not 945. The peak assigned to $[Cu_2(patH_2)(CO_3)]$ was by far the most intense peak in the spectrum. Increasing the base concentration from 2 to 3 and 4 equiv or increasing reaction times increases the intensity of peaks attributed to $[Cu_2(patH_2)(CO_3)]$, present as the H^+, Na^+, and NEt_3H^+ adducts.

The presence of CO_3^{2-}, presumed to arise from atmospheric CO_2 absorbed by the basic solutions, was established by using

(30) Pilbrow, J. R.; Hanson, G. R. *Methods Enzymol.* **1993**, *227*, 330.

natural-abundance or ^{13}C-enriched Na_2CO_3 instead of triethylamine and a copper(II) salt which contains a poor coordinating anion, copper(II) triflate (though copper(II) nitrate is equally as good), to prepare the binuclear copper(II) complex $[Cu_2(patH_2)(CO_3)]$. A comparison of the peaks attributed to $[Cu_2(patH_2)(^{12}CO_3)Na]^+$ (Figure 8b) and $[Cu_2(patH_2)(^{13}CO_3)Na]^+$ (Figure 8c) reveals the expected one mass unit difference proving that carbonate is indeed present in this binuclear copper(II) complex. Similar effects were also observed for the peaks attributed to the hydrogen ion and triethylammonium adducts. When copper(II) chloride was employed in this reaction the most intense peak occurred at m/z 935 Da (Figure S6). This peak was assigned to the binuclear copper(II) complex $[Cu_2(patH_2)Cl]^+$ rather than $[Cu_2(patH_2)(H_2O)(OH)]^+$ on the basis of a comparison of the theoretical isotope distributions for these two complexes with that observed experimentally (Figure S6). This peak persisted even at very high orifice potentials (OR = 100 V), testimony to the very high stability of the species, possibly a chloride-bridged binuclear copper(II) complex. In contrast the peaks at m/z = 952.2 and 973.2 attributed to the mono- and diaqua adducts of $[Cu_2(patH_2)Cl]^+$ only persist at intermediate orifice potentials suggesting that the two water molecules are either solvated or axially coordinated to the copper(II) ions. Initially (time ~ 5 min) there was no evidence for the formation of any carbonate species.

The combined results obtained from mass spectrometry and the electronic absorption, CD, and EPR spectral titrations, for the formation of the binuclear copper(II) patellamide D complexes, are consistent with the following equilibria:

$$[Cu(MeOH)]^{2+} + patH_4 + NEt_3 \rightleftharpoons [Cu(patH_3)]^+ + NEt_3H^+$$

$$[Cu(patH_3)]^+ + [Cu(MeOH)]^{2+} + NEt_3 \rightleftharpoons [Cu_2(patH_2)]^{2+} + NEt_3H^+$$

$$[Cu_2(patH_2)]^{2+} + NEt_3 \rightleftharpoons [Cu_2(patH_2)(OH)]^+ + NEt_3H^+$$

$$[Cu_2(patH_2)(OH)]^+ + CO_2 \rightleftharpoons [Cu_2(patH_2)(CO_3)] + H_3O^+ \quad (10)$$

where $[Cu(patH_3)]^+$ represents the multiple mononuclear complexes present in solution (eq 6). The binuclear copper(II) complex formed after the addition of 2 equiv of base ($[Cu_2(patH_2)]^{2+}$) may have either chloride or water in the fourth equatorial coordination site. The complex formed after 3 equiv of base was added is formulated as having a hydroxide ion coordinated to one of the copper(II) ions ($[Cu_2(patH_2)(OH)]^+$), as it could represent an intermediate in the fixation of carbon dioxide to form carbonate.[31] The most thermodynamically stable complex in solution, $[Cu_2(patH_2)(CO_3)]$, is fully formed after 3 or more equiv of triethylamine has been added and the solution left standing for at least 2–3 days. The equilibria consistent with the formation of $[Cu_2(patH_2)(CO_3)]$ when Na_2CO_3 replaces triethylamine are

$$[Cu(MeOH)]^{2+} + patH_4 + CO_3^{2-} \rightleftharpoons [Cu(patH_3)]^+ + HCO_3^-$$

$$[Cu(patH_3)]^+ + [Cu(MeOH)]^{2+} + HCO_3^- \rightleftharpoons [Cu_2(patH_2)]^{2+} + H_2CO_3$$

$$[Cu_2(patH_2)]^{2+} + CO_3^{2-} \rightleftharpoons [Cu_2(patH_2)(CO_3)] \quad (11)$$

Structure of the Copper(II) Patellamide D Complexes. Although patellamide D has a twisted "figure eight" (type III) conformation in the solid state, dissolution in methanol may produce a square conformer (type II) in which there are no hydrogen bonds or a rectangular form (type I) which is stabilized by two intramolecular hydrogen bonds.[9,11] There are eight nitrogen atoms in the macrocyclic ring where copper(II) can potentially bind to consecutive thiazole, deprotonated peptide amide, and oxazoline nitrogens. While computer simulation of the X- and S-band EPR spectra of $[Cu(patH_3)]^+$ have established the copper(II) ions' coordination sphere as involving a set of three nitrogens, Q-band spectra reveal the presence of multiple species. The multiple species ($[Cu(patH_3)X]^+$ and $[Cu(patH_3')X]^+$, X = Cl, H_2O) can arise through from different ligands (Cl, H_2O) in the fourth equatorial coordination site and the binding of copper(II) ions to one or more of the four potential binding sites within the asymmetric patellamide D molecule.

Electronic absorption, CD, and EPR spectral titrations in conjunction with mass spectrometry have established the formation of three binuclear copper(II) patellamide D complexes ($[Cu_2(patH_2)]^{2+}$, $[Cu_2(patH_2)(OH)]^+$, and $[Cu_2(patH_2)(CO_3)]$). Computer simulations of the EPR spectra (Figures 6 and 7) have provided the internuclear copper(II)–copper(II) distances and the relative orientation of the two copper(II) sites in these binuclear complexes (Table 2). Interestingly, in addition to the changes in symmetry of the binuclear copper(II) complex the internuclear copper(II)–copper(II) distance decreases from 6.8 to 4.8 Å and, finally, to 3.7 Å. Dreiding models of $patH_4$ indicate that it is possible to bind two copper(II) ions that are 6.8 Å apart, but in order for this to occur all four transannular N–H···O hydrogen bonds must be broken. Consequently the decrease in the internuclear copper(II)–copper(II) distance from 6.8 to 4.8 to 3.7 Å as $[Cu_2(patH_2)]^{2+}$ is converted to $[Cu_2(patH_2)(OH)]^+$ and then to $[Cu_2(patH_2)(CO_3)]$ may be a result of refolding the two halves of the patellamide molecule in such a way as to bring the two copper ions closer together. The g and A matrices, values of ξ, η, and τ, and the internuclear distance for $[Cu_2(patH_2)(CO_3)]$ correspond to those observed for a crystal of the structurally characterized $[Cu_2(ascidH_2)(1,2\text{-}\mu\text{-}CO_3)(H_2O)_2]\cdot 2H_2O$ complex dissolved in methanol, indicating that the carbonate anion also bridges the two copper(II) ions bound to $patH_2$.[14] As discussed in a future paper,[14] the shorter copper(II)–copper(II) distance and the change in symmetry of the $[Cu_2(ascidH_2)(1,2\text{-}\mu\text{-}CO_3)(H_2O)_2]\cdot 2H_2O$ complex in solution (3.6 Å, axial symmetry) versus the solid state (4.43 Å, triclinic symmetry) may arise from a change in the structure of the bridging group. Interestingly, copper(II)–copper(II) distances of 3.6 and 4.7 Å have been observed in the tetrameric copper(II) complex $[Cu_4(dpt)_4(CO_3)Cl_2]^{4+}$ (dpt = bis(3-aminopropyl)amine), where CO_3^{2-} is at the center of a rectangle of copper(II) ions and bridges the four copper sites with a single oxygen atom between two copper(II) ions.[32] Thus, in solution there may be a 1,1-μ-CO_3 bridge between the two copper(II) ions bound to patellamide D. The bridging ligand (CO_3^{2-}) presumably stabilizes the $[Cu_2(patH_2)(CO_3)]$ complex, which is the most thermodynamically stable species in solution. A reasonable structure for the binuclear $[Cu_2(patH_2)(CO_3)]$ complex is depicted in **4**.

There are two mechanisms which can account for the formation of carbonate from carbon dioxide. In the first mechanism (eq 10) the binuclear copper(II) patellamide complexes play a role in CO_2 fixation, while, in the second mechanism, triethylamine may deprotonate water present in the methanolic solutions producing hydroxide which can undergo nucleophilic addition to CO_2 forming carbonate. Carbonate can then coordinate to the

(31) Kitajima, N.; Fujisawa, K.; Koda, T.; Hikichi, S.; Moro-oka, Y. *J. Chem. Soc., Chem. Commun.* **1990**, 1357.

(32) Einstein, F. W. B.; Willis, A. C. *Inorg. Chem.* **1981**, *20*, 609.

binuclear copper(II) patellamide complex (eq 11). The existence of a third end point in the electronic absorption, CD, and EPR spectral titrations of solutions containing copper(II) chloride and $patH_4$ in a two to one ratio with triethylamine support the former mechanism as the deprotonation of water by triethylamine in solution would not affect the spectral properties of $[Cu_2(patH_2)]^{2+}$. In addition the mass spectrum of a solution containing $patH_4$, copper(II) chloride, and triethylamine in the ratio of 1:2:3 revealed a peak at $m/z = 945.0$, which was observed to increase with time. The assignment of this peak to $[Cu_2(patH)(CO_2)]^+$ also supports the first mechanism. A rigorous assignment of the mechanism for CO_2 fixation requires further experimentation, which is currently in progress.

Acknowledgment. This work was supported by Grants A28931377 and NSRG-21 awarded by the Australian Research Council and The University of Queensland, respectively. We thank the National Biomedical ESR Center in Milwaukee, WI, for the use of their S-band EPR spectrometer and W. E. Antholine for assistance in obtaining these spectra; this Center is funded through NIH Grant RR-01008.

Supplementary Material Available: Figure S1, showing (a) the EPR spectrum of a solution containing 1 equiv of copper(II) chloride and patellamide D in methanol, (b) the EPR spectrum of copper(II) chloride in methanol, and (c) a spectral subtraction (a–b) generating the spectrum attributed to $[Cu(patH_3)]^+$, Figure S2, showing a mass spectrum of a solution containing 1 equiv of $^{63}CuCl_2 \cdot 2H_2O$, patellamide D, and triethylamine, with an inset of an expansion of the peak $m/z = 975$ together with the two theoretical isotope distributions for $[Cu(patH_3)Cl \cdot (NEt_3H)]^+$ and $[Cu(patH_3)(H_2O)(OH)(NEt_3H)]^+$, Figure S3, showing X-band EPR spectra of $[Cu(patH_3)]^+$ including (a) the first-derivative EPR spectrum in methanol, $\nu = 9.2537$ GHz, (b) the second-derivative EPR spectrum, and (c) a computer simulation of (b), LSE = 9.78×10^{-3}, Figure S4, showing EPR spectra of $[Cu_2(patH_2)(OH)]^+$ prepared using copper(II) chloride including (a) an X-band experimental spectrum showing the $\Delta M_s = \pm 1$ resonances, $\nu = 9.2983$ GHz, (b) a computer simulation of (a), LSE = 9.913×10^{-3}, (c) an X-band experimental spectrum showing the $\Delta M_s = \pm 2$ resonances, $\nu = 9.2976$ GHz, and (d) a computer simulation of (c), LSE = 3.180×10^{-2}, Figure S5, showing EPR spectra of $[Cu_2(patH_2)(CO_3)]$ prepared using copper(II) nitrate including (a) an X-band experimental spectrum showing the $\Delta M_s = \pm 1$ resonances, $\nu = 9.2974$ GHz, (b) a computer simulation of (a), LSE = 1.162×10^{-2}, (c) an X-band experimental spectrum showing the $\Delta M_s = \pm 2$ resonances, $\nu = 9.2965$ GHz, and (d) a computer simulation of (c), LSE = 5.367×10^{-2}, and Figure S6 showing a mass spectrum of a solution containing $^{63}CuCl_2 \cdot 2H_2O$, patellamide D, and sodium carbonate in the ratio 2:1:2, with an inset of an expansion of the $m/z = 935$ peak together with the theoretical isotope distributions for $[Cu_2(patH_2)Cl]^+$ and $[Cu_2(patH_2)(H_2O)(OH)]^+$ (6 pages). Ordering information is given on any current masthead page.